Eur. J. Mineral.
2017, **29**, 1055–1066
Published online 9 June 2017

A re-investigation of ardealite from the type locality, the "dry" Cioclovina Cave (Şureanu Mountains, Romania)

Delia-Georgeta DUMITRAŞ*

Department of Mineralogy (INI), Geological Institute of Romania, 1 Caransebeş Str., 012271 Bucharest, Romania
*Corresponding author, e-mail: d_deliaro@yahoo.com

Abstract: Material from the type locality, the "dry" Cioclovina Cave, Şureanu Mountains, Romania, was re-examined in order to update the descriptive mineralogy of ardealite, a rare hydrated calcium acid phosphate sulfate. Ardealite from Cioclovina has a S/P ratio ranging between 1/0.87 and 1/0.98. Although S remains the main tetrahedral cation in the structure, P is consistently present at concentrations between 19.10 and 20.45 wt% P_2O_5 (0.928–0.992 P atom per formula unit). Concerning the other cations, the mineral shows a very restricted range of composition, without Fe and with very low Mn, Mg, Na and K contents. The indices of refraction are $\alpha = 1.530(2)$, $\beta = 1.537(2)$ and γ (calculated for $2V_\gamma = 86°$) = 1.543. The measured density [$D_m = 2.335(3)$–$2.342(5)$ g/cm^3] agrees well with the calculated values [$D_x = 2.317$–2.350 g/cm^3]. The average unit-cell parameters refined from 31 sets of X-ray powder diffraction data are $a = 5.719(5)$, $b = 31.012(28)$, $c = 6.249(7)$ Å and $\beta = 117.21(6)°$. Thermally assisted X-ray diffraction analyses confirm that water is lost in three steps; the loss of molecular water is a two-step process and is complete below 250 °C. The first thermal breakdown products are brushite and bassanite. The band multiplicity on the IR-absorption spectrum ($3\nu_3 + 1\nu_1 + 3\nu_4 + 2\nu_2$) suggests that the protonated phosphate and sulfate groups have C_s point symmetry. The mineral derives from the reaction between calcium carbonate from the moonmilk flows or the cave floor and phosphoric solutions derived from bat guano, with or without hydroxylapatite as a precursor, at pH values up to 5.5.

Key-words: ardealite; hydrated calcium acid phosphate sulfate; physical properties; crystal chemistry; unit-cell parameters; thermal behavior; infrared spectrum; authigenesis; "dry" Cioclovina Cave; Romania.

1. Introduction

Ardealite, a rather rare hydrated calcium acid phosphate sulfate [$Ca_2(HPO_4)(SO_4)\cdot 4H_2O$], was first described and named by Schadler (1932) from the fossil bat-guano deposit in the "dry" Cioclovina Cave (Şureanu Mountains, Romania), following the identification of a new species by Halla (1931). This was the first report of this mineral in the cave environment. The discovery of ardealite was the direct result of the early mining in the area, conducted for the precious guano fertilizer. Subsequently, ardealite has been reported from more than 20 other caves (Hill & Forti, 1997), including six new occurrences in Romania (*e.g.*, Dumitraş, 2009).

Ardealite has received little attention and only a few complete analyses were reported in the literature; several aspects of its structure and crystal chemistry remain unclear. Halla (1931) determined its optical properties, unit-cell dimensions and possible space groups; he also noted the similarity between its properties and those of brushite and gypsum, and proposed the isostructurality of these mineral species.

The physical properties and chemical composition of type ardealite are well described by Schadler (1932) and probably by Hill & Hendriks (1936), but the subsequent studies of ardealite from Cioclovina were mainly of a reconnaissance nature, and no comprehensive mineralogical data are available. Currently, little is known of its thermal and infrared behavior or compositional variation. In spite of a relatively large number of new occurrences, the chemistry of the mineral has not been sufficiently studied, owing to the small particle size, the common intergrowths with other phases, and the analytical difficulties. One of the principal aims of this work was therefore to shed light on these aspects, by investigation of the chemical variability and particularly of the extent of the substitution of $(HPO_4)^{2-}$ by $(SO_4)^{2-}$ in ardealite from the type locality. In the process, investigations of some other caves in the South Carpathians revealed numerous additional occurrences and material therein was used for comparison. This study was also undertaken in order to supplement previous partial descriptions, to fully characterize the mineral, and to give a thorough description of its chemistry, physical properties, crystallographic data, and thermal and infrared behavior.

2. Geological setting

The "dry" Cioclovina cave, located near the homonymous small village in the Şureanu Mountains (about 16 km east-southeast of Haţeg, the major town in the area), is

DOI: 10.1127/ejm/2017/0029-2655
0935-1221/17/0029-2655 $ 5.40

developed in Tithonian–Neocomian algal micritic limestones with calcarenite levels, which form the Haţeg Basin (the upper part of Jurassic deposits, Fig. S1 in Supplementary Material linked to this article and freely available online on the GSW website of the journal: http://eurjmin.geoscienceworld.org/). It represents the upper (fossil) level of a karstic system that also includes a water-laden cave, namely the "wet" Cioclovina, which is part of the Ponorici-Cioclovina cu Apă karstic system (7890 m in length). The altitude of the entrance is 775 m. A detailed description of the cave and of its topography was recently given by Tomuş (1999), from which was taken the longitudinal sketch in Fig. S1.

The cave contained an outstanding volume of bat guano: a quantity of 23 000 tons of this fertilizer was mined out during the first half of the 20th century (Bleahu *et al.*, 1976). The mined part of the cave consists in a nearby subhorizontal gallery with some short divergent passages, measuring on the whole about 900 m. This portion was used for the sampling of the specimens used for this study (Fig. S1).

Since the pioneering work of Schadler (1929) on the guano deposit, many comprehensive mineralogical studies on the composing phosphate minerals have been carried out (*e.g.*, Constantinescu *et al.*, 1999; Marincea *et al.*, 2002; Marincea & Dumitraş, 2003; Dumitraş *et al.*, 2008; Dumitraş, 2009), although it is now becoming apparent that the mineralogy is very complex and includes many rare mineral species. The cave is the type locality for ardealite but is also known for the occurrence of a rich mineral association, including, at the level of the guano deposit: tinsleyite, taranakite, monetite, crandallite, leucophosphite, variscite, francoanellite, gypsum, bassanite, calcite, vaterite, aragonite, hematite, goethite, birnessite, romanèchite, todorokite, quartz, illite and kaolinite (*e.g.*, Dumitraş, 2009). Some exotic mineral species such as berlinite, burbankite, churchite-(Y), chlorellestadite, foggite, paratacamite (atacamite), collinsite, sampleite and kröhnkite were reported by Onac *et al.* (2002, 2011) but some of these species were probably misidentified (Marincea & Dumitraş, 2005).

Ardealite is one of the minor components of the guano deposit, occurring however in most of the phosphate-bearing samples. Beside hydroxylapatite and brushite, it formed the base of the huge mass of guano extracted from the cave. Actually, the mineral accounts for up to 5 vol% of the guano deposit in the cave.

3. Analytical procedures

Because the crystals of ardealite are very small and notoriously unstable under the electron beam, the bulk methods of analysis were preferred. A wavelength-dispersive electron-microprobe study was, however, attempted. The apparatus used was a CAMECA SX-50, and the following conditions were used: excitation voltage 15 kV, specimen current 20 nA, beam size 5 μm, peak count-time 10 s, and background count-time 20 s. The electron beam was defocused to 15 μm, and the samples were moved during the analysis to minimize the thermal decomposition of mineral, but the instability of the sample under the beam prevented good acquisitions.

The analytical procedures and specifications for wet-chemical analysis, X-ray powder diffraction study (XRD), inductively coupled plasma atomic-emission spectrometry (ICP-AES) and thermal analysis are similar to those described by Marincea *et al.* (2002) and Dumitraş *et al.* (2008). Samples were prepared for analysis by hand-picking bunches of crystals, crushing them with two or three downward strokes in a mortar and removing any obvious contaminant from the powder. The purified separate was crushed, lightly ground in acetone and then dried, rapidly etched with cold 0.01 N acetic acid, abundantly washed with water, and again air dried.

For the ICP-AES analysis, aliquots of 0.2 g of finely pulverized sample were dissolved with 6 mL of concentrated (65%) HCl, boiled until drying, removed with 20 mL of HCl 2 M and then analyzed.

Observations of the crystal morphologies were conducted using a JEOL JSM-840 scanning electron microscope (SEM). Attempts to acquire energy-dispersive spectra (EDS) were made using a Tracor Northern TN-2000 system, for 100 s (live time), with an accelerating voltage of 10 kV and a beam current of 10 nA. The X-ray spectra were collected and processed with the PGT semiquantitative software. Full ZAF corrections were applied to the raw X-ray data, but the results were of very poor quality due to the burn-up of the samples. Samples were found to be enough beam-sensitive to prevent the acquisition of good quality SEM patterns at high magnification.

XRD analysis was performed on a Siemens D-5000 Kristalloflex automated diffractometer equipped with a graphite diffracted-beam monochromator (Cu$K\alpha$ radiation, $\lambda = 1.54056$ Å). The analytical conditions were the same as described by Dumitraş *et al.* (2004). The unit-cell parameters were calculated by least-squares refinement of the XRD data, using the computer program of Appleman & Evans (1973) modified by Benoit (1987). Synthetic silicon (NBS 640b) was used as an external standard.

High-temperature XRD was performed using a Brucker (AXS) D8 Advance diffractometer, under a constant helium flow (20 mL/min flow rate). The powders were deposited on a platinum holder [$a = 3.9231(5)$ Å at 25 °C]. The heating rate was of 10 °C/min, and each record was made 10 min after the desired temperature was attained. At each temperature step the sample was equilibrated for 15 min. Three Pt lines belonging to the holder (at ~2.265, 1.962 and 1.826 Å) were used to correct for shift to the main lines, assuming the same expansivity for all the phases.

The infrared absorption spectra were recorded using both a SPECORD M-80 spectrometer, in the frequency range 250–4000 cm^{-1} (Marincea & Dumitraş, 2003), and a Fourier-transform THERMO NICOLET NEXUS spectrometer, in the frequency range 400–4000 cm^{-1}. In both cases, standard pressed disk techniques and KBr pellets were used.

Indices of refraction were measured without heating, using calibrated oils, a spindle stage and a classical JENAPOL-U microscope.

4. Mode of occurrence and morphology of the crystals

Macroscopically, ardealite occurs as earthy masses of chalky, porous, appearance. The macroscopic color is snow white to yellowish white, the same as from brushite (Dumitraş *et al.*, 2004). Under the optical microscope, the ardealite masses appear as extremely fine-grained spherule-coated surfaces that hardly allow recognition of any single aggregate.

The SEM study shows that ardealite from Cioclovina is generally associated with hydroxylapatite and brushite occurring as: (1) irregular lining of hydroxylapatite bunches of crystals or partial fillings of veinlets or cracks affecting the hydroxylapatite mass; (2) partial or complete filling of intergranular microcavities (from hundreds of μm to 3 mm across) in the hydroxylapatite aggregates; (3) overgrowths on brushite aggregates, in which the textural relationships clearly show that ardealite postdates brushite; and (4) sprays or crusts of ardealite crystals, up to 0.5 cm thick, associated or not with brushite, occurring on the hydroxylapatite masses from the cave floor. This fourth textural type is the most frequent in the present phosphate association from Cioclovina. The composing ardealite aggregates form efflorescence-like clusters of up to 0.5 cm in diameter, disposed on successive layers. The EDS microprobe analyses revealed that a S-rich Ca phase, probably gypsum, locally develops as veins or nests in the ardealite mass.

The SEM examination of micromounts showed that the ardealite masses are generally composed by sheaf-, cluster-like or rarely by radiating aggregates of crystals to a diameter of 0.2 mm. Closer inspection reveal the presence of minute pseudo-prismatic or platy crystals of micrometric sizes, arranged in radiating groups to a diameter of 0.2 mm, which form cabbage-like or rosette-like aggregates (Fig. 1A and B). The compact radial groups are generally built up of thin blades or individual crystals with the **c*** axis pointing outwards from the center. Locally, they are composed by many "butterfly"-like interlocking or loosely packed aggregates of crystals, up to 100 μm in length (Fig. 1C and D). This kind of aggregate was synthesized by Rinaudo & Abbona (1988) and Rinaudo *et al.* (1994) and consists of two systems of interlaced laths, which radiate from a common center in opposite directions. The common center of a "butterfly"-like aggregate may be an unusual twin of ardealite with reentrant angles, with two individuals developed from the tips, the same as observed in the case of brushite by Abbona *et al.* (1993).

The habit of individual crystals can be described as lamellar, with crystals elongated along [0 0 1] and tabular on (0 1 0). Even if the poor quality of the very small crystals limited the gathered information, the habit of the mineral seems to be very similar to that of synthetic brushite (Rinaudo *et al.*, 1994); the forms recognized are {0 1 0}, {1 1 1} and $\{1\,1\,\bar{1}\}$.

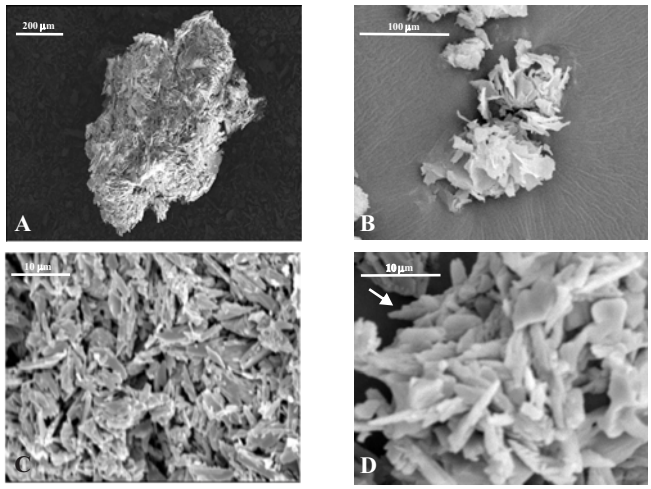

Fig. 1. SEM pictures of typical ardealite aggregates. (A) Cabbage-like aggregates of platy crystals. (B) Monomineralic mass of platy crystals, showing the rosette-like radial development of the composing aggregates. (C) Aggregate of randomly oriented interlocking and subparallel platy, partly fractured, crystals of ardealite. (D) Detail on a mass of flakes of ardealite. The arrow indicates the termination of a "butterfly-like" aggregate.

5. Physical properties

Macroscopically, ardealite occurs as damp, off-white to pale yellow earthy masses of chalky appearance, whose luster is pearly but less pronounced than that of brushite. The hardness is the same as from brushite and gypsum: an estimation based on abrasion of talc and gypsum surfaces indicates a reasonable value of 2 on Mohs scale. There is no discernible fluorescence under either short-wave (254 nm) or long-wave (366 nm) ultraviolet radiation. It is noteworthy that the mineral gave slight fluorescence under Cu$K\alpha$ radiation, even on short exposures of up to 1 h duration.

The mineral was examined in immersion oils with a petrographic microscope but, because of the extremely fine-grained nature of the material and the composite nature of the crystals, little information could be obtained. The measurement of the refraction indices of the mineral was difficult, in view of the very small size of the crystals. For this reason, the indices of refraction were measured on stacks of platy subparallel crystals as maximum and minimum values, respectively. They are $n_{min} = \alpha = 1.530(2)$ and $n_{max} = \beta = 1.537(2)$, resulting in $\gamma_{calc} = 1.543$. The optical angle could be measured with difficulty owing to the minute size of the crystals, but a value $2V_{\gamma} = 86°$ was measured on a "butterfly"-like aggregate and used to calculate the γ value. The $2V_{\gamma}$ value is identical with that given by Balenzano *et al.* (1984) for ardealite from La Guangola Cave.

Density determination on five separate clusters, using a Berman balance and toluene as displacement fluid, at 20 °C, gave an average measured value $D_m = 2.342(5)$ g/cm^3.

Table 1. Bulk chemical analyses of selected samples of ardealite from Cioclovina.

Sample	D 37 A[a]	D 53 A[a]	D 31[b]	D 35 A[b]	D 35 B[b]	D 37 B[b]	D 53 B[b]
Crt. no.	1	2	3	4	5	6	7
K_2O	0.03	0.06	0.08	0.05	0.06	0.05	0.07
Na_2O	0.06	0.00	0.05	0.06	0.07	0.06	0.04
CaO	32.18	32.39	32.45	32.45	32.46	32.46	32.45
MnO	0.02	0.01	0.00	0.01	0.00	0.01	0.01
MgO	0.02	0.02	0.01	0.02	0.01	0.01	0.02
P_2O_5	19.80	19.10	19.13	19.56	19.62	20.45	19.26
SO_3	23.80	24.80	24.92	24.44	24.36	23.43	24.78
H_2O[c]	23.63	23.27	23.36	23.41	23.42	23.53	23.37
Total	99.54	99.65	100.00	100.00	100.00	100.00	100.00
Number of ions on the basis of 2 (S + P) and 8 (O) in the anhydrous part of the formula							
K	0.002	0.004	0.006	0.004	0.004	0.004	0.005
Na	0.007	0.000	0.006	0.008	0.008	0.007	0.004
Ca	1.992	1.996	1.993	1.992	1.993	1.993	1.993
Mn	0.001	0.000	0.000	0.000	0.000	0.000	0.000
Mg	0.002	0.002	0.001	0.002	0.001	0.001	0.002
$(HPO_4)^{2-}$	0.968	0.930	0.928	0.949	0.952	0.992	0.934
$(SO_4)^{2-}$	1.032	1.070	1.072	1.051	1.048	1.008	1.066
Degree of hydration (water molecules *pfu*)							
H_2O	4.069	3.998	4.000	4.000	4.000	4.000	4.000

[a] Wet-chemical analyses.
[b] ICP-AES analyses.
[c] In the ICP-AES analyses, as calculated for stoichiometry.

The mean density of 10 separate clusters taken from the same sample was also measured by sink-float in methylene iodide diluted with toluene, at 20 °C, and is $D'_m = 2.335(3)$ g/cm^3. Both measured densities are higher than the value of 2.30 g/cm^3 given by Schadler (1932) for the type material, but agrees better with the calculated densities, based on the chemical formulae (Table 1) and the unit-cell parameters (Table 2), accepting $Z = 4$ (Sakae *et al.*, 1978): $D_x = 2.317$–2.350 g/cm^3 (Table 3).

Calculations based on the Gladstone–Dale relationship were performed using the chemical data, the calculated densities and the mean index of refraction (Table 3). From these calculations, the compatibility indices range from 0.005 to 0.023, indicating, according to Mandarino (1981), superior (four cases) and excellent (three cases) compatibilities. The refractive indices depend strongly on the water content of the mineral, which may to some extent explain the spread of the calculated values of the mean refractive index based on the Gladstone–Dale rule (Table 3).

6. Chemical data

Only a few wet-chemical analyses were published before (*i.e.*, Schadler, 1932, and apparently Hill & Hendriks, 1936, who analyzed ardealite from "Transylvania"), hence two new analyses were performed and included in Table 1. Microanalysis was also tried but the results were poor. The preliminary qualitative chemical investigation, carried out by EDS during attempts for SEM observation, revealed that the mass of ardealite contains abundant Ca, P, S; no other significant cation was detected. Fluorine and chlorine were sought but not detected. Wavelength-dispersive EMP analyses were also attempted. Prior to analysis, thin sections were prepared by setting dispersed samples in epoxy on glass slides. The attempts to analyze the mineral by this method gave poor results owing to the burn-up of the sample and the lifting of the carbon coat under vacuum. The decrepitation under vacuum results from the weak H-bonding of the H_2O groups to the $(HPO_4)^{2-}$ and $(SO_4)^{2-}$ anions. Fast analyses using a defocused beam of 20 μm in diameter, while reducing the beam-damage effects, did not eliminate them, resulting in non-stoichiometric formulae.

More fortunate were the ICP-AES analyses, obtained after selective dissolution: the results obtained for five analyses are given in Table 1 (analyses 3–7). The values issued from direct measurements of CaO were accurate to within ±1.3%. For all the compositions given in Table 1, H_2O^+ and H_2O^- were assumed to be present in stoichiometric concentrations.

Both wet-chemical and ICP-AES analyses in Table 1 were normalized to 2 (S + P) and 8 (O) atoms in the anhydrous part of the formula. The basis for normalization was chosen in order to be consistent with the structure refinement of Sakae *et al.* (1978). Some minor elements were also analyzed by ICP-AES and are given in Table 4.

If one considers the analyzed samples in terms of their composition (Tables 1 and 4) a number of features become apparent: (1) The extent of substitution of K, Na, Mn and Mg for Ca is negligible in all of the samples, summing up to 0.70% of the sites normally occupied by Ca. Iron was not detected. Analyses for other minor elements (Table 4)

Table 2. Unit-cell parameters of selected samples of ardealite from Cioclovina.

Sample	a (Å)	b (Å)	c (Å)	β (°)	V (Å^3)	n[a]	N[b]
2217 A	5.725(2)	30.993(8)	6.252(3)	117.08(2)	987.6(6)	3	78
2217 B	5.723(2)	31.113(8)	6.259(2)	117.23(2)	991.1(4)	10	87
D 2 B	5.721(2)	30.994(9)	6.253(2)	117.28(2)	983.8(4)	4	65
D 2 C	5.720(2)	31.018(9)	6.242(2)	117.27(2)	984.4(5)	6	48
D 7 A	5.726(1)	30.995(7)	6.243(2)	117.28(1)	984.7(3)	6	51
D 9 B	5.723(2)	30.999(8)	6.251(2)	117.20(2)	986.3(4)	5	50
D 22 B	5.709(3)	30.968(9)	6.252(5)	117.19(3)	983.2(8)	6	57
D 31 A	5.721(5)	30.990(9)	6.245(9)	117.23(1)	984.6(1)	4	73
D 35 A	5.720(2)	31.014(9)	6.255(3)	117.24(2)	986.6(5)	5	105
D 35 B	5.717(2)	31.019(9)	6.254(3)	117.18(2)	986.5(5)	5	103
D 35 C	5.725(4)	31.041(8)	6.238(4)	117.31(3)	985.1(7)	7	51
D 35 D	5.716(1)	30.988(7)	6.242(2)	117.23(1)	982.9(3)	7	58
D 36 D	5.717(1)	31.007(6)	6.247(1)	117.20(1)	984.7(2)	10	48
D 37 A	5.721(2)	30.995(9)	6.248(3)	117.25(2)	984.8(5)	6	88
D 37 B	5.713(2)	31.031(9)	6.233(3)	117.09(2)	983.9(5)	9	95
D 45 A	5.719(2)	31.034(9)	6.247(3)	117.26(2)	985.7(5)	8	104
D 47 B	5.723(2)	30.995(7)	6.254(2)	117.25(1)	986.1(3)	5	94
D 53 A	5.736(2)	31.024(9)	6.263(2)	117.26(2)	990.8(4)	7	85
D 59 B	5.716(2)	31.021(8)	6.254(3)	117.22(2)	986.2(5)	4	73
D 59 C	5.718(2)	31.016(9)	6.250(2)	117.14(2)	986.4(5)	6	74
D 59 D	5.716(2)	31.013(9)	6.248(3)	117.23(2)	984.9(4)	7	96
D 59 E	5.724(2)	31.014(9)	6.242(3)	117.25(2)	985.0(5)	5	70
D 63 B	5.714(3)	30.973(9)	6.261(4)	117.09(3)	986.5(7)	5	68
D 63 C	5.716(2)	30.991(9)	6.258(3)	117.09(2)	986.9(5)	5	101
D 66 B	5.721(2)	30.977(8)	6.249(2)	117.27(1)	984.3(4)	5	60
D 121 B	5.717(2)	30.998(9)	6.248(2)	117.24(2)	984.4(4)	4	48
D 121 C	5.710(1)	31.065(8)	6.241(2)	117.20(1)	984.5(3)	9	43
D 131 B	5.721(3)	31.012(9)	6.251(4)	117.23(3)	986.1(6)	4	81
D 131 C	5.720(2)	31.037(8)	6.246(3)	117.25(2)	985.8(6)	4	64
D 131 D	5.716(2)	31.034(9)	6.240(3)	117.15(2)	984.8(6)	6	62
D 196 A	5.712(2)	31.003(9)	6.248(3)	117.13(3)	984.8(7)	5	42

[a] Number of refining cycles.
[b] Number of reflections in the 2θ range 10–76° used for refinement.

Table 3. Physical parameters of selected samples of ardealite from Cioclovina.

Sample	M[a]	V[b]	D_x[c]	K_C[d]	D'_x[e]	$\overline{n}_X$[f]	K_P[g]	$1-(K_P/K_C)$[h]
D 31 A	344.443	984.564	2.323	0.2270	2.366	1.527	0.2312	−0.0185
D 35 A	344.331	986.589	2.317	0.2271	2.365	1.526	0.2318	−0.0207
D 35 B	344.346	986.537	2.318	0.2265	2.371	1.524	0.2317	−0.0230
D 37 A	348.610	984.836	2.350	0.2276	2.359	1.533	0.2289	−0.0057
D 37 B	347.176	983.891	2.342	0.2273	2.362	1.532	0.2293	−0.0088
D 47 B	344.319	986.145	2.318	0.2270	2.366	1.526	0.2317	−0.0207
D 53 A	346.133	990.773	2.320	0.2270	2.366	1.527	0.2315	−0.0198

[a] Molecular mass.
[b] Cell volume (Å^3).
[c] Calculated density.
[d] Chemical molar refractivity.
[e] Density calculated according to the Gladstone–Dale law, using the mean index of refraction ($\overline{n} = 1.537$), and the chemical molar refractivity.
[f] $\overline{n}_X = D_x \cdot K_C + 1$.
[g] Physical molar refractivity, $K_P = (\overline{n} - 1)/D_x$.
[h] Compatibility index according to Mandarino (1981).

failed to identify substantial concentrations of these. As in the case of brushite (Dumitraş *et al.*, 2004) and hydroxylapatite (Dumitraş *et al.*, 2008), ardealite from Cioclovina contains less Ba than Sr. The REE contents are relatively low. According to partial analyses in Table 4, ardealite from Cioclovina is enriched in the light REE relative to heavy REE + Y: all but one samples respect this rule, which also parallels the behavior of brushite (Dumitraş *et al.*, 2004) and hydroxylapatite (Dumitraş *et al.*, 2008). In addition to these elements, trace

Table 4. Trace-element contents of selected samples of ardealite from Cioclovina (ppm).

Sample	Sr	Ba	Cu	V	Cr	Ni	La	Ce	Eu	Y	Yb
D 31	10.0	8.77	31.0	1.55	3.3	5.5	2.66	0.00	0.23	1.82	0.07
D 35 A	10.0	2.17	32.0	1.92	2.8	12.0	0.00	0.00	0.25	1.24	0.00
D 35 B	4.8	0.88	18.0	1.10	2.1	7.4	0.15	7.82	0.14	0.87	0.01
D 37 B	12.0	1.43	9.2	1.15	1.4	3.7	3.18	2.47	0.17	0.19	0.00
D 53 B	39.0	20.0	17.0	2.34	4.3	5.4	1.73	0.00	0.16	0.76	0.00

concentrations of some transition metals (*i.e.*, Cu, V, Cr and Ni) were also identified but are very minor. (2) From the analyses in Table 1, it results that ardealite from Cioclovina has always S > P (*apfu*). A problem arises from the fact that this statement is based on bulk ICP-AES and wet-chemical analyses, with no indication of the sample purity excepting the XRD tests. Care was taken to avoid including other phases, but the presence of small amounts of brushite or gypsum in some of the samples cannot be ruled out. Small amounts of these minerals may subsist in the handpicked powders since the separation of the two minerals is practically impossible owing to their extremely fine grain size. An environmental SEM study is in progress and will offer an answer to the problem. (3) Whereas all of the formulae deduced in Table 1 approximate the ideal composition $Ca_2(HPO_4)(SO_4)\cdot 4H_2O$, none of them is in exact stoichiometric agreement. The S:P ratio is far to be constantly equal to 1:1, which supports the existence of a solid solution along the binary join brushite–gypsum, as first suggested by Halla (1931) and confirmed by synthesis experiments (see below). In fact, among the synthesis experiments carried out in the system $CaO–SO_3–P_2O_5–H_2O$ (*e.g.*, Sakae *et al.*, 1978; Aslanian *et al.*, 1980; Aslanian & Stoilova, 1982; Rinaudo & Abbona, 1988; Rinaudo *et al.*, 1994, 1996; Pinto *et al.*, 2012), only two (Sakae *et al.*, 1978; Aslanian & Stoilova, 1982) have succeeded in producing stoichiometric "ardealite" with a S:P ratio of 1:1. As expected, there is a strong negative correlation between the P and S contents of the samples in Table 1 (also Fig. 2). The results of analyses in Table 1 indicate that ardealite from Cioclovina has consistently S > P. The $(SO_4)^{2-}/(HPO_4)^{2-}$ molar ratios (S/P) vary from 1/0.87 to 1/0.98, in contrast with the previous data published by Schadler (1932), that is, S/P = 1/1.16 or Hill & Hendriks (1936), that is, S/P = 1/1.15. Concerning the other literature data, only the analysis of Maki & Kashima (1977) of ardealite from the Onino-Iwaya Cave (Japan) gave a supra-unitary S/P ratio (1/0.85), whereas the mean S/P ratio reported for ardealite samples from La Guangola Cave (Italy) is 1/1.06 (Balenzano *et al.*, 1984), and 1/1.04 for those from Mereşti Cave (Romania, Marincea *et al.*, 2004). The maximum amount of S observed in our samples corresponds to 53.6% occupancy of the tetrahedral site, and is far to indicate a limit of the S-for-P substitution in the structure of ardealite, since Rinaudo & Abbona (1988) reported successful syntheses of ardealite-like phases with S/P = 0.7.

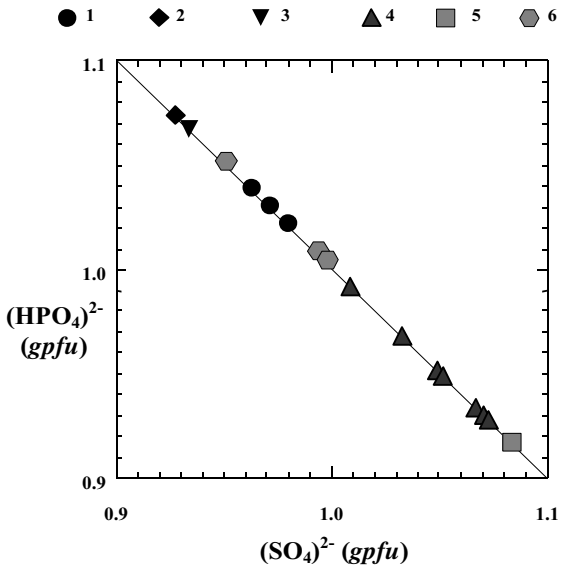

Fig. 2. Variations of $(SO_4)^{2-}$ as a function of $(HPO_4)^{2-}$ contents in ardealite. The contents are expressed in S and P atoms per formula unit. The sample symbols represent: (1) La Guangola Cave, Italy (Balenzano *et al.*, 1984); (2) Cioclovina Cave, Romania (Schadler, 1932); (3) an unknown location in Transylvania, probably Cioclovina (Hill & Hendriks, 1936); (4) Cioclovina Cave, Romania (present work); (5) Onino-Iwaya Cave, Japan (Maki & Kashima, 1977); and (6) Mereşti (Marincea *et al.*, 2004). (Online version in color.)

7. X-ray powder diffraction data

The X-ray powder diffraction pattern of ardealite is similar to, although distinguishable from that of synthetic $Ca_2(HPO_4)(SO_4)\cdot 4H_2O$ obtained by Sakae *et al.* (1978). In all our patterns, at least four medium-to-strong lines, centered at about 4.30, 4.10, 3.15 and 2.95 Å, could not be indexed nor could be related to any known impurity if we accept the crystallization of ardealite in the centrosymmetric space group *Cc* proposed by Sakae *et al.* (1978). In fact, the XRD patterns of ardealite from Cioclovina are virtually identical to that reported by a number of authors for natural ardealite (*e.g.*, Balenzano *et al.*, 1984; Marincea *et al.*, 2004; Frost *et al.*, 2012). The four supplementary lines may in fact indicate a lower true symmetry for ardealite, which would be in agreement with the assumptions of Aslanian & Stoilova (1982) or Frost *et al.* (2012) that the true space group of ardealite is *Cm*. Similar lines were identified by Rinaudo & Abbona (1988) and Rinaudo *et al.* (1994) in the diffraction patterns of synthetic $Ca_2(SO_4)_{1-x}(HPO_4)_x\cdot 4H_2O$ com-

pounds, with $0.15 < x < 0.70$. A Rietveld refinement of the structure, based on X-ray powder data, is in progress, and will be the subject of a further paper.

Cell parameters of 31 representative samples are given in Table 2. The differences between the cell parameters in Table 2 probably account for differences in the hydration degree of the samples. The mean values, obtained as average of all parameters in the table are $a = 5.719(5)$, $b = 31.012(28)$, $c = 6.249(7)$ Å and $\beta = 117.21(6)°$. These cell parameters agree well with recent values obtained for ardealite from other localities (*e.g.*, Balenzano *et al.*, 1984; Marincea *et al.*, 2004), but notably differ from the early set determined by Halla (1931) for ardealite from Cioclovina ($a = 5.67$, $b = 29.28$, $c = 6.28$ Å and $\beta = 113.83°$ accepting that the cell determined by this author has the β angle of gypsum, as also supposed by Palache *et al.*, 1951). Taking into account that the assumption of Palache *et al.* (1951) was based on the hypothesis of the presence in ardealite of a strong subcell having $b' = b/2$ and also that the older measurements have poor accuracy, the values derived by Palache *et al.* (1951) are fair. Both individual and mean values in Table 2 are in good agreement with those reported by Sakae *et al.* (1978) for synthetic $Ca_2(HPO_4)(SO_4)\cdot 4H_2O$ [$a = 5.721(5)$, $b = 30.992(5)$, $c = 6.250(4)$ Å and $\beta = 117.26(6)°$].

Statistical treatment of the data in Tables 1 and 2 shows increases of a, c, β and V cell parameters with increasing $(SO_4)^{2-}$-for-$(HPO_4)^{2-}$ substitution (the correlation coefficients being +0.42, +0.86, +0.30 and +0.66, respectively), whereas a small but significant decrease in the b parameter with increasing S content was recorded (correlation coefficient −0.35). At least regarding the cell volume, this finding is surprising, since in compounds having monoclinic symmetry, the cell volume V increases from gypsum to brushite and therefore correlates with the $^{[4]}$P content.

8. Thermal decomposition

Thermal studies of natural ardealite samples were reported by Balenzano *et al.* (1984) and Frost *et al.* (2012) and gave an accurate view on the thermal behavior of this mineral. The weight loss corresponding to the loss of molecular water occurred in two steps: between 25 and ~215 °C (two water molecules) and between ~215 and ~225 °C (another two water molecules). The loss of water begins at room temperature because some of H_2O groups are only weakly H-bonded to the $(HPO_4)^{2-}$ and $(SO_4)^{2-}$ anions. After the loss of all the molecular water at ~225 °C (Frost *et al.*, 2012) the mineral decomposes. This behavior, proposed by Frost *et al.* (2012), was verified, in the case of ardealite from Cioclovina, by X-ray-assisted heating. The evolution of the sample during heating is depicted in Fig. 3.

The X-ray powder diffraction experiments indicate that the framework structure is retained upon the first dehydration step, whereas the second leads to the breakdown into brushite + bassanite, not into $Ca_2(HPO_4)(SO_4)\cdot 2H_2O$ as supposed by Frost *et al.* (2012). The obtained brushite has $a = 5.808(3)$, $b = 15.227(14)$, $c = 6.233(5)$ Å and $\beta = 116.11(4)°$, whereas bassanite has $a = 12.027(9)$, $b = 6.327(6)$, $c = 12.674(9)$ Å and $\beta = 90.23(3)°$ – both of them at room temperature. The ideal decomposition reaction can be written as: $Ca_2(HPO_4)(SO_4)\cdot 4H_2O \rightarrow Ca(HPO_4)\cdot 2H_2O + Ca(SO_4)\cdot 0.5H_2O + 1.5\ H_2O$, then the loss of water below 200 °C is less important than calculated by Frost *et al.* (2012), being of up to 1.5 molecules, in good agreement with the findings of Balenzano *et al.* (1984).

As expected, and in agreement with the structural refinements of Sakae *et al.* (1978), during heating up to 100 °C, the progressive loss of water combined with the thermal expansion of the lattice conduce to a progressive decrease of the a and c cell parameters and to an increase of the larger b parameter (Table 5). At 150 °C, ardealite is still persistent, but the loss of water leads to a reduced crystallinity (Fig. 3) and to contraction of the lattice (Table 5). In order to optimize the internal consistency of the data, lattice parameters obtained during heating were scaled to the unit-cell parameters obtained at room temperature.

The crystalline breakdown products at 250 °C, resulting from the complete removal of molecular water predicted by Frost *et al.* (2012) at ~225 °C, were relict bassanite [$a = 11.999(1)$, $b = 6.392(6)$, $c = 12.901(3)$ Å and $\beta = 90.19(6)°$] and γ-anhydrite [$a = 6.990(6)$, $c = 6.252(5)$ Å]. The lack of any phosphate is not surprising, since at ~220 °C monetite issued from the dehydration of brushite incipiently dehydrates and transforms into amorphous calcium pyrophosphate, according to the reaction $2CaHPO_4 = Ca_2P_2O_7 + H_2O$ (Dumitraş *et al.*, 2004).

The complete dehydration occurred at 350 °C, the sole recognizable phases on the XRD pattern being a poorly crystallized γ-anhydrite [$a = 6.982(2)$, $c = 6.354(5)$ Å], and recrystallized β-$Ca_2P_2O_7$ [$a = 6.684(3)$, $c = 24.145(9)$ Å], which is still recognizable at 450 °C. On the contrary, at 450 °C, the transition of γ-anhydrite (hexagonal) to β-anhydrite (orthorhombic) is complete, as correctly predicted by West & Sutton (1954). The cell parameters of this new product are $a = 6.993(6)$, $b = 7.009(6)$, $c = 6.232(5)$ Å, registering minor variations until 600 °C.

The partial loss of sulfur, recorded by Frost *et al.* (2012) at ~565 °C, does not influence the breakdown products at 750 °C, which are β-anhydrite and whitlockite [$a = 10.338(9)$, $c = 37.143(9)$ Å], probably resulting from the partial decomposition of hydroxylapatite, present as impurity in the initial sample (Fig. 3). Poorly crystallized whitlockite and β-anhydrite are still persistent in the quenched product (Fig. 3).

9. Infrared absorption data

Figure 4 displays the infrared absorption spectra obtained for three representative samples of ardealite from Cioclovina with and without a Fourier-transform spectrometer, whereas Table 6 gives the wavenumbers, characters and intensities of the infrared absorption bands, as well as tentative band assignments. The positions of the

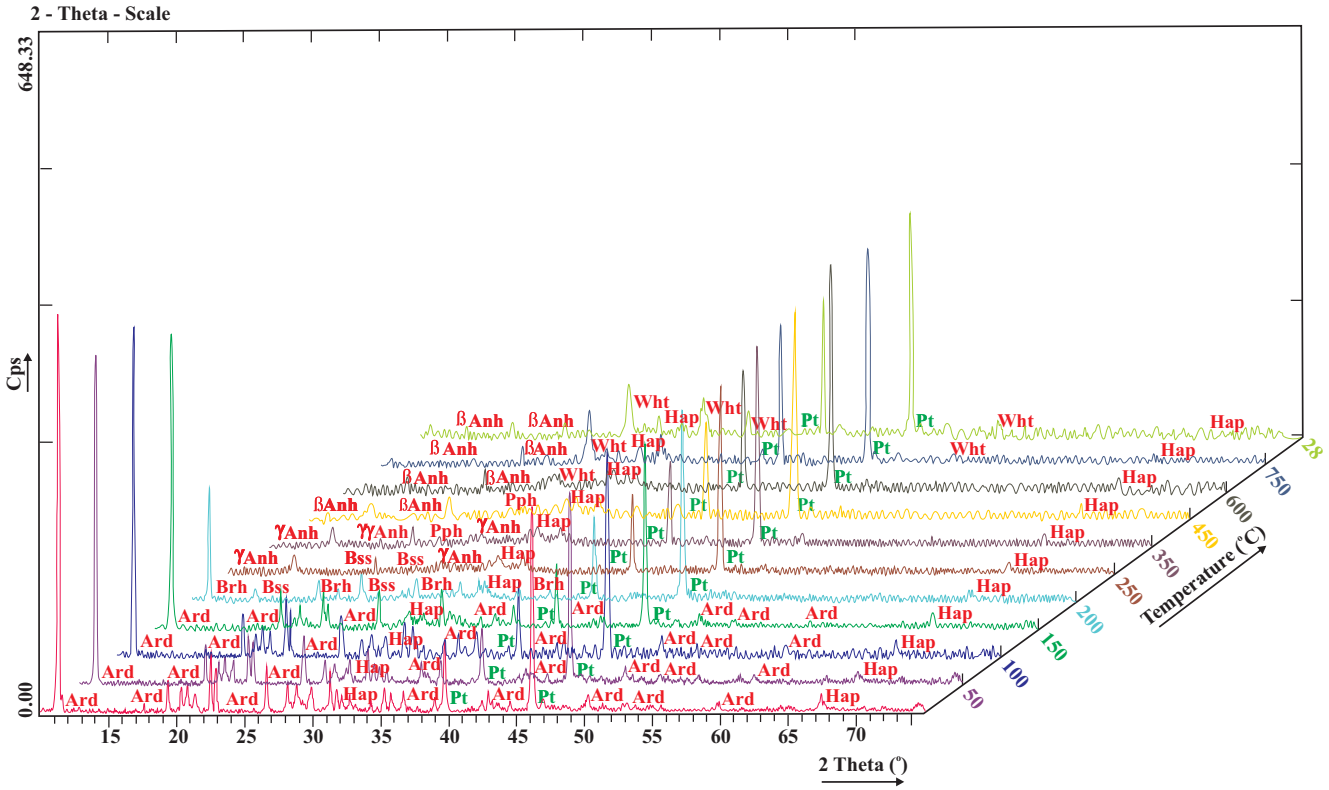

Fig. 3. X-ray powder patterns of a representative sample of ardealite from Cioclovina (sample D 53), as a function of temperature. Representative lines of platinum (Pt), ardealite (Ard), hydroxylapatite (Hap), brushite (Brh), bassanite (Bss), anhydrite (Anh), Ca pyrophosphate (PPh) and whitlockite (Wht) are marked. (Online version in color.)

Table 5. Evolution of the cell parameters of Cioclovina ardealite during heating.[a]

T (°C)	a (Å)	b (Å)	c (Å)	V (Å^3)	n[b]	N[c]
25	5.736(2)	31.024(9)	6.263(2)	990.8(4)	3	45
50	5.730(3)	31.029(11)	6.253(2)	988.6(5)	5	40
100	5.724(3)	31.111(17)	6.247(3)	991.1(6)	6	43
150	5.732(4)	30.997(16)	6.240(4)	986.8(8)	9	38

[a] Determined by least-squares refinement of 50 reflections in the 2θ range 5–70°.
[b] Number of least-squares refining cycles.
[c] Number of unrejected reflections used for refinement.

bands in Table 6 were established each as the mean of the wavenumbers recorded for similar bands in four different spectra of representative samples, with standard deviations given in brackets.

There are only three bands clearly recognizable in the OH-stretching region between 3000 and 4000 cm^{-1}, although the structure determination by Sakae *et al.* (1978) shows that in synthetic $Ca_2(HPO_4)(SO_4)\cdot 4H_2O$ there are four hydrogen bonds implying the water molecules in the structure, then four theoretical absorption bands in the range. According to the bond-distance *vs.* frequency correlation of Libowitzky (1999), the nominal frequencies of these bands must occur in the range of 3188–3550 cm^{-1}, in agreement with the OH···O distances of 2.70–3.00 Å found by structure analysis by Sakae *et al.* (1978). The three bands in our spectra occur specifically in this frequency range. Two of the bands due to the stretching vibrations of molecular water consequently overlap.

As well as in brushite (Curry & Jones, 1971) and as observed by Marincea *et al.* (2004), a fifth hydrogen bond seem to be established between OH groups pertaining to the protonated phosphate groups, which could explain the presence, in our spectra, of the shoulder at ~2970 cm^{-1}. This could explain the six absorption bands resolved by Frost *et al.* (2011) in the region of water stretching.

The presence of two crystallographically distinct H_2O molecules, as indicated by the results of the crystal structure analysis (Sakae *et al.*, 1978), explains the pronounced splitting of the H–O–H bending motions of molecular water: the didentate bending at ~1720 cm^{-1} and the broad complex composed of six bands, centered at ~1640 cm^{-1}. As correctly observed by Frost *et al.* (2011), the bands at ~1720 cm^{-1} could be assigned to strongly hydrogen-bonded water molecules, whereas the complex of bands at ~1640 cm^{-1} is due to weakly hydrogen-bonded water.

The fundamental frequencies of the tetrahedral molecular groups $(SO_4)^{2-}$ and $(HPO_4)^{2-}$ are, for a T_d punctual symmetry, as follows: 981 cm^{-1} (ν_1), 451 cm^{-1} (ν_2), 1104 cm^{-1} (ν_3) and 613 cm^{-1} (ν_4) for sulfate (Müller & Krebs, 1967) and 980 cm^{-1} (ν_1), 363 cm^{-1} (ν_2), 1082 cm^{-1} (ν_3) and 515 cm^{-1} (ν_4) for protonated phosphate (Bhatnagar, 1968). The bands due to the $(SO_4)^{2-}$ and $(HPO_4)^{2-}$ ν_1

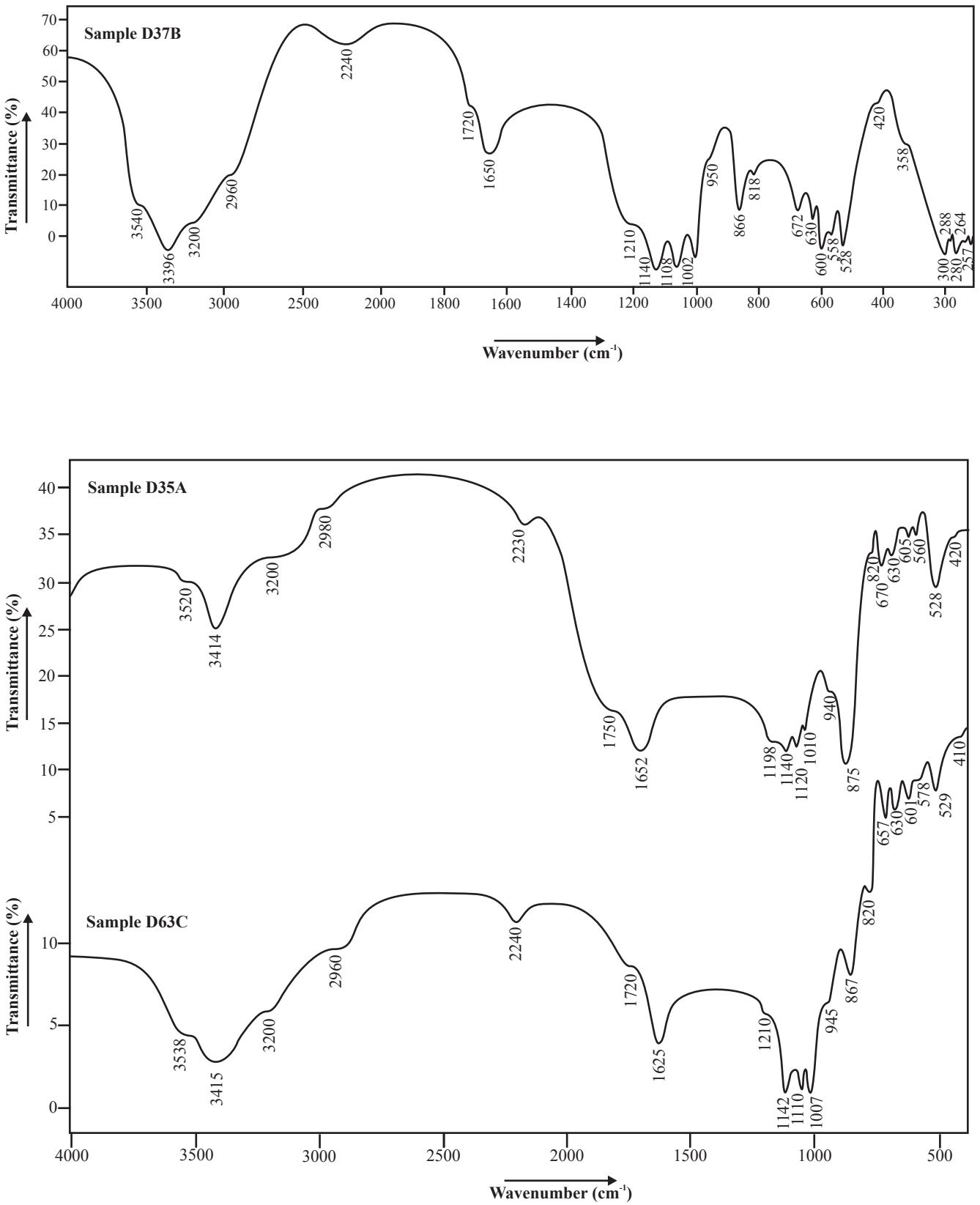

Fig. 4. Infrared spectra of three selected samples of ardealite from Cioclovina: IR spectrum (top) and FTIR spectra (bottom).

Table 6. Position and assignment of the infrared absorption bands recorded for selected samples of ardealite from Cioclovina.[a]

Structural group	Vibrational mode	Wavenumber (cm^{-1})[b]	Wavenumber (cm^{-1})[c]	Character, intensity[d]
H_2O	ν_3 antisymmetric stretching	3552(28)	3529(7)	vs, shd
H_2O	ν'_3 antisymmetric stretching	3396(15)	3402(17)	vs, b
H_2O	ν_1 symmetric stretching	3205(10)	3195(10)	vs, shd
$(HPO_4)^{2-}$	(P)O–H stretching	2958(5)	2963(24)	s, shd
$(HPO_4)^{2-}$	(P)O–H stretching	2240(8)	2235(6)	w, b
H_2O	ν_4 in-plane H–O–H bending	1718(5)	1738(15)	m, b[e]
H_2O	ν'_4 in-plane H–O–H bending	1640(18)	1640(11)	s, b[f]
$(HPO_4)^{2-}$	P–O–H in-plane bending	1209(6)	1206(10)	m, shd
$(HPO_4)^{2-}$, $(SO_4)^{2-}$	ν_3 O–P(S)–O antisymmetric stretching	1142(2)	1140(1)	vs, b
$(HPO_4)^{2-}$, $(SO_4)^{2-}$	ν'_3 O–P(S)–O antisymmetric stretching	1101(7)	1115(6)	vs, b (shd)
$(HPO_4)^{2-}$, $(SO_4)^{2-}$	ν''_3 O–P(S)–O antisymmetric stretching	1003(1)	1009(2)	vs, sh
$(HPO_4)^{2-}$, $(SO_4)^{2-}$	ν_1 O– P(S)–O symmetric stretching	956(8)	947(10)	m, shd
$(HPO_4)^{2-}$	P–O(H) symmetric stretching	867(5)	873(4)	s, sh
$(HPO_4)^{2-}$	P–O–H out-of-plane bending	821(3)	820(1)	m, b (shd)
$H_2O + (SO_4)^{2-}$	ν_2 H–O–H + ν_4 O–S–O	671(1)	664(7)	m, sh
$H_2O + (SO_4)^{2-}$	ν'_2 H–O–H + ν'_4 O–S–O	627(6)	633(5)	m, sh
$(HPO_4)^{2-} + (SO_4)^{2-}$	ν_4 O–P–O + ν''_4 O–S–O	600(3)	604(2)	s, b
$(HPO_4)^{2-}$	ν'_4 O–P–O in-plane bending	559(3)	570(9)	s, b (shd)
$(HPO_4)^{2-}$	ν''_4 O–P–O in-plane bending	526(4)	529(1)	s, sh (shd)
$(HPO_4)^{2-}$, $(SO_4)^{2-}$	ν_2 O–P(S)–O out-of-plane bending	418(5)	414(8)	w, shd
$[CaO_6(H_2O)_2]^{10-}$, $(SO_4)^{2-}$	ν'_2 O–S–O + lattice mode (+ H–O–H ?)	360(5)	–	m, shd
$[CaO_6(H_2O)_2]^{10-}$	Lattice mode (Ca–O)	304(3)	–	s, sh
$[CaO_6(H_2O)_2]^{10-}$	Lattice mode (Ca–O)	289(1)	–	s, sh (shd)
$[CaO_6(H_2O)_2]^{10-}$	Lattice mode (Ca–O)	280(2)	–	s, sh
$(HPO_4)^{2-}$	ν'_2 O–P–O out-of-plane bending	265(3)	–	s, sh (shd)
$[CaO_6(H_2O)_2]^{10-}$	Lattice mode (Ca–O)	256(3)	–	s, sh (shd)

[a] Assumptions made by analogy with brushite and taking into account the work of Aslanian & Stoilova (1982), Rinaudo & Abbona (1988) and Frost *et al.* (2011).
[b] IR records, means of the values recorded for the samples D 37 A, D 37 B, D 47 B, and D 53 A; standard deviations into brackets.
[c] FTIR records, means of the values recorded for the samples D 35 A, D 35 B, D 59 D, and D 63C.
[d] s = strong; m = medium; w = weak; vs = very strong; sh = sharp; b = broad; and shd = shoulder.
[e] Split into two bands.
[f] Broad complex, split into six distinct absorption bands.

and ν_3 fundamentals must consequently overlap, whereas ν_2 and ν_4 will be presumably distinct. As compared with the spectra recorded for brushite (*e.g.*, Dumitraş *et al.*, 2004), the spectra of ardealite show characteristic broader absorption bands in the stretching region of protonated phosphate; it results that the hypothesis of an overlap of the $(SO_4)^{2-}$ and $(HPO_4)^{2-}$ stretching bands is sustained. The strong broad absorption near 1200 cm^{-1}, perceived as a shoulder in Fig. 4, is in the same position and, deconvoluted, of the same strength and profile as the distinctive absorption band ascribed by Dumitraş *et al.* (2004) and Marincea *et al.* (2004) to the P–O–H in-plane bending of the $(HPO_4)^{2-}$ groups in brushite. In addition, the IR-absorption spectrum of ardealite is characterized by a splitting of the ν_3 (XO_4) fundamentals into three well-resolved bands at ~1140, 1100 and 1005 cm^{-1}, indicating distorted (XO_4) tetrahedrons for both sulfate and protonated phosphate groups.

Absorption bands in the remainder of the spectra could not be unequivocally assigned due to the large overlapping of lattice modes, phosphate bendings and P–O–H librations. Detailed assignment of the bending bands ν_2 and ν_4 is consequently difficult but comparison with brushite might help at least distinguishing the characteristic bands associated with protonated phosphate bendings. Such bands are tentatively given in Table 6. If the assignments in Table 6 are correct, the band multiplicity ($3\nu_3 + 1\nu_1 + 3\nu_4 + 2\nu_2$) is consistent with a C_s point symmetry of the protonated phosphate; assuming the same point symmetry for the sulfate groups, we must find the same band multiplicity in the case of ν_4 and ν_2 fundamentals.

10. Genetic considerations

As well as in other guano-bearing caves (*e.g.*, Peştera Mare de la Mereşti – Marincea *et al.*, 2004), part of the ardealite from Cioclovina seems to be in the result of a crystallization sequence from hydroxylapatite to brushite and finally ardealite. Both direct precipitation from an acid solution and formation by replacement of brushite may be proposed, but closer examination reveals that many brushite aggregates are partly replaced by ardealite. Some S-bearing veins fill fractures of the brushite aggregates but, because of their small sizes (usually <10 μm) and of the volatility of the sample under the electron beam, there are some difficulties in the identification of the composing mineral species, just assumed to be ardealite. Properly identified ardealite is commonly present as overgrowths on brushite aggregates and, in all cases, textural relationships are conclusive for an early formation of brushite. It

results that the hypothesis of formation of ardealite through step-by-step replacement of preexistent brushite may be favored at Cioclovina. This is consistent with progressive crystallization under open-system conditions within fractures affecting brushite masses, due to incoming acidic sulfate-rich solutions.

The presence of $(SO_4)^{2-}$ in solution is clearly critical for the formation of ardealite. The sulfate ions in the leaching waters, which are strongly acidic, may derive both from the oxidation of the pyrite-bearing schists and sedimentary formations upstream and from the oxidation of the organic matter in the guano itself. A higher sulfur imprint if characteristic for the lower Senonian deposits of the Haţeg Basin, where Laufer (1924) reported gypsum infillings on the fissures that affect the Fizeşti sandstone. Part of the sulfate can also derive from direct alteration of the bat guano, as established by Pogson *et al.* (2011) on the basis of isotope studies at Jenolan Caves (Australia). Experimental data (*e.g.*, Aslanian & Stoilova, 1982; Rinaudo & Abbona, 1988; Rinaudo *et al.*, 1994; Pinto *et al.*, 2012), as well as geochemical evidence, suggest that, at pH values of 4–5.5 and constant compositions, an ardealite-like phase can nucleate. A direct precipitation of gypsum and ardealite instead of brushite from sulfate-bearing acidic solutions is favored by the fact that at acidic values of pH (less than 7.2), phosphate is stable as $(H_2PO_4)^-$, precluding the formation of brushite instead of a sulfate-bearing phase. This implies that, at Cioclovina, local pH variations and the sulfur availability were the mean factors to determine the crystallization of ardealite.

The pH variations are probably related to the partial dissolution of carbonates, which produces volatile CO_2 and neutralizes the strongly acidic phosphoric or sulfatic solutions. The source for all the other elements in the ardealite structure is mainly the surrounding carbonate mass. This assumption is supported by the fact that ardealite (average REE + Y = 4.78 ppm), as well as brushite (average REE + Y = 4.75 ppm according to Dumitraş *et al.*, 2008) and hydroxylapatite (average REE + Y = 12.79 ppm according to Dumitraş *et al.*, 2008) have low REE + Y contents, which indicate a remobilization from carbonates rather than from REE-richer *terra rossa*. In fact, these contents are much lower than those recorded in 10 selected samples of carbonates from the limestone country-rock and from the solidified moonmilk flows on the walls, which range from 21.00 to 34.19 ppm (average 25.28 ppm).

Acknowledgements: I express my thanks to Prof. Dr. Emil Constantinescu, former President of Romania, who kindly communicated some of the samples, IR, thermal and XRD analyses used for this study. Fruitful discussions on the field with Professors André-Mathieu Fransolet, Essaïd Bilal, and Ştefan Marincea are highly appreciated. The author sincerely thank Dr. Jacques Moutte (Ecole Nationale Supérieure des Mines de Saint-Etienne – ENSMSE) for kindly supplying the ICP-AES analysis, M. Olivier Valfort (ENSMSE) for technical assistance during the thermally assisted X-ray powder work, Dr. Frédéric Hatert (Université de Liège) for assistance in carrying out the FTIR analyses. Field assistance by Mr. Bogdan Tomuş is gratefully acknowledged. The quality of this contribution was improved after a careful review by Drs. Ştefan Marincea and Frédéric Hatert. The author is grateful to the Chief Editor Patrick Cordier for handling the manuscript, as well as to two anonymous referees for their thorough reviews of an earlier draft. Part of the logistical support necessary for this study was offered through three research projects funded by the Romanian Ministry of Education and Research (Contracts 113/15.10.2001, 4-153/04.11.2004, and PN-II-ID-PCE-2011-3-0023). The Rhône-Alpes Region is gratefully acknowledged for financing part of the research work by allowing a MIRA grant to the author, in 2005–2006.

References

Abbona, F., Christenson, F., Franchini Angela, M., Lundager Madsen, H.E. (1993): Crystal habit and growth conditions of brushite, $CaHPO_4{\cdot}2H_2O$. *J. Cryst. Growth*, **131**, 331–346.

Appleman, D.E. & Evans Jr., H.T. (1973): Indexing and least-squares refinement of powder diffraction data. U.S. Geol. Surv. Comput. Contrib. 20 (NTIS Doc. PB-216).

Aslanian, S. & Stoilova, D. (1982): Étude de l'ardéalite, membre intermédiaire du système gypse-brushite. *Bull. Minéral.*, **105**, 621–624.

Aslanian, S., Stoilova, D., Petrova, R. (1980): Isodimorphe substitution in $CaSO_4$–$CaHPO_4$–H_2O-system. *Z. Anorg. Allgem. Chem.*, **465**, 209–220.

Balenzano, F., Dell'Anna, L., Di Piero, M., Fiore, S. (1984): Ardealite, $CaHPO_4CaSO_4{\cdot}4H_2O$: a new occurrence and new data. *N. Jb. Miner. Mh.*, 1984, 363–372.

Benoit, P.H. (1987): Adaptation to microcomputer of the Appleman-Evans program for indexing and least-squares refinement of powder-diffraction data for unit-cell dimensions. *Am. Mineral.*, **72**, 1018–1019.

Bhatnagar, V.M. (1968): Infrared spectra of hydroxyapatite and fluorapatite. *Bull. Soc. Chim. France*, **1968**, 1771–1773.

Bleahu, M., Decu, V., Negrea, S., Pleşa, C., Povară, I., Viehmann, I. (1976): Caves from Romania. Ştiinţifică şi Enciclopedică Ed., Bucharest, 413 p. (in Romanian).

Constantinescu, E., Marincea, S., Crăciun, C. (1999): Crandallite in the phosphate association from Cioclovina cave (Şureanu Mts., Romania). *in* "Mineralogy in the system of earth sciences", E. Constantinescu, ed. Imperial College Press, London, 1–5.

Curry, N.A. & Jones, D.W. (1971): Crystal structure of brushite, calcium hydrogen orthophosphate dihydrate: a neutron-diffraction investigation. *J. Chem. Soc. A*, 3725–3729.

Dumitraş, D.G. (2009): Mineral associations in the sediments from the "dry" Cioclovina Cave. Ed. "Thèses à la carte", Villeneuve d'Ascq, France, 320 p., http://www.diffusiontheses.fr/ (in Romanian).

Dumitraş, D.G., Marincea, Ş., Fransolet, A.M. (2004): Brushite in the bat guano deposit from the "dry" Cioclovina Cave (Şureanu Mountains, Romania). *N. Jb. Miner. Abh.*, **180**, 45–64.

Dumitraş, D.G., Marincea, Ş., Bilal, E., Hatert, F. (2008): Apatite-(CaOH) in the fossil bat guano deposit from the "dry" Cioclovina Cave, Şureanu Mountains, Romania. *Can. Mineral.*, **46**, 431–445.

Frost, R.L., Palmer, S.J., Henry, D.A., Pogson, R. (2011): A Raman spectroscopic study of the "cave" mineral ardealite $Ca_2(HPO_4)(SO_4){\cdot}4H_2O$. *J. Raman Spectrosc.*, **42**, 1447–1454.

Frost, R.L., Palmer, S.J., Pogson, R. (2012): Thermal stability of the "cave" mineral ardealite $Ca_2(HPO_4)(SO_4)\cdot 4H_2O$. *J. Therm. Anal. Calorim.*, **107**, 549–553.

Halla, F. (1931): Isomorphe Beziehungen und Doppelsalzbildung zwischen Gips und Brushit. *Z. Kristallogr.*, **80**, 349–352.

Hill, C. & Forti, P. (1997): Cave minerals of the world, 2nd edn. National Speleological Society, Hunstville, Alabama, 239 p.

Hill, C. & Hendriks, S. (1936): Composition and properties of superphosphate. *Ind. Eng. Chem*., **28**, 440–447.

Laufer, F. (1924): Contributions to the geological study of the neighbourhood of the Haţeg city. *Ann. Inst. Geol. Rom.*, **10**, 301–333 (in Romanian).

Libowitzky, E. (1999): Correlation of O–H stretching frequencies and O–H···O hydrogen bond lengths in minerals. *Monatsh. Chem.*, **130**, 1047–1059.

Maki, T. & Kashima, N. (1977): Chemical composition of some cave phosphate minerals. *J. Jpn. Assoc. Mineral. Petrol. Econ. Geol*., **72**, 181–187.

Mandarino, J.A. (1981): The Gladstone–Dale relationship. IV. The compatibility concept and its application. *Can. Mineral.*, **19**, 441–450.

Marincea, Ş. & Dumitraş, D. (2003): The occurrence of taranakite in the "dry" Cioclovina Cave (Şureanu Mountains, Romania). *N. Jb. Miner. Mh.*, **2003**, 127–144.

—, — (2005): First reported sedimentary occurrence of berlinite ($AlPO_4$) in phosphate-bearing sediments from Cioclovina Cave, Romania – Comment. *Am. Mineral.*, **90**, 1203–1208.

Marincea, Ş., Dumitras, D., Gibert, R. (2002): Tinsleyite in the "dry" Cioclovina Cave (Sureanu Mountains, Romania): the second world occurrence. *Eur. J. Mineral*., **14**, 157–164.

Marincea, Ş., Dumitraş, D.G., Diaconu, G., Bilal, E. (2004): Hydroxylapatite, brushite and ardealite in the bat guano deposit from Peştera Mare de la Mereşti, Perşani Mountains, Romania. *N. Jb. Miner. Mh.*, **2004**, 464–488.

Müller, A. & Krebs, B. (1967): Normal coordinate treatment of XY_4-type molecules and ions with T_d symmetry. Part I. Force constants of a modified valence force field and of the Urey–Bradley force field. *J. Mol. Spectrosc*., **24**, 180–197.

Onac, B.P., Breban, R., Kearns, J., Tămaş, T. (2002): Unusual minerals related to phosphate deposits in Cioclovina Cave, Sureanu Mountains (Romania). *Theor. Appl. Karst*., **15**, 27–34.

Onac, B.P., Effenberger, H.S., Collins, N.C., Kearns, J.B., Breban, R.C. (2011): Revisiting three minerals from Cioclovina Cave (Romania). *Int. J. Speleol.*, **40**, 99–108.

Palache, C., Berman, H., Frondel, C. (1951): The system of mineralogy, Vol. II. John Wiley & Sons, New York, NY, 1124 p.

Pinto, A.J., Carneiro, J., Katsikopoulos, D., Jiménez, A., Prieto, M. (2012): The link between brushite and gypsum: miscibility, dehydration, and crystallochemical behavior in the $CaHPO_4\cdot 2H_2O$–$CaSO_4\cdot 2H_2O$ system. *Cryst. Growth Des.*, **12**, 445–455.

Pogson, R.E., Osborne, A.L., Colchester, D.M., Cendon, D.I. (2011): Sulfate and phosphate speleothems at Jenolan Caves, New South Wales, Australia. *Acta Carstol.*, **40**, 239–254.

Rinaudo, C. & Abbona, F. (1988): A contribution to the study of the crystal chemistry of calcium sulfate phosphate hydrate. *Miner. Petrogr. Acta*, **31**, 95–105.

Rinaudo, C., Lanfranco, A.M., Franchini-Angela, M. (1994): The system $CaHPO_4\cdot 2H_2O$–$CaSO_4\cdot 2H_2O$: crystallizations from calcium phosphate solutions in the presence of SO_4^{2-}. *J. Cryst. Growth*, **142**, 184–192.

Rinaudo, C., Lanfranco, A.M., Boistelle, R. (1996): The gypsum-brushite system: crystallization from solutions poisoned by phosphate ions. *J. Cryst. Growth*, **158**, 316–321.

Sakae, T., Nagata, H., Sudo, T. (1978): The crystal structure of synthetic calcium phosphate-sulfate hydrate, Ca_2HPO_4-$SO_4\cdot 4H_2O$ and its relation to brushite and gypsum. *Am. Mineral*., **63**, 520–527.

Schadler, J. (1929): Mineralogische-petrographische Characteristik der Phosphat-ablagerung in der Cioclovinahöhle bei Pui. *Pub. Muz. Hunedoara*, **5**, 1–3.

— (1932): Ardealit, ein neues Mineral $CaHPO_4\cdot CaSO_4 + 4H_2O$. *Zb. Mineral. A*, 40–41.

Tomuş, R.B. (1999): The karst complex Ciclovina. The basin 2063. Proteus Ed., Hunedoara, 55 p. (in Romanian).

West, R.R. & Sutton, W.J. (1954): Thermography of gypsum. *J. Am. Ceram. Soc.*, **37**, 221–224.

Received 24 March 2016
Modified version received 11 December 2016
Accepted 26 May 2017